Mild Hydrothermal Synthesis of the Complex Hafnium Containing Fluorides $Cs_2[M(H_2O)_6][Hf_2F_{12}]$ (M= Ni, Co, and Zn), $CuHfF_6(H_2O)_4$ and $Cs_2Hf_3Mn_3F_{20}$ Based on HfF_7 and HfF_6 Coordination Polyhedra

Gyanendra B. Ayer, Vladislav V. Klepov, Mark D. Smith, and Hans-Conrad zur Loye*

Department of Chemistry and Biochemistry, University of South Carolina,
631 Sumter St., Columbia, SC, United States
*e-mail: zurloye@mailbox.sc.edu

Abstract

A series of new Hf(IV) containing fluorides with three different compositions, $Cs_2[M(H_2O)_6][Hf_2F_{12}]$ (M = Ni, Co, and Zn), $CuHfF_6(H_2O)_4$ and $Cs_2Hf_3Mn_3F_{20}$, were synthesized as high quality single crystals via a mild hydrothermal route. The compounds with compositions of $Cs_2[M(H_2O)_6][Hf_2F_{12}]$ (M = Ni, Co, and Zn) and $CuHfF_6(H_2O)_4$ crystallize in the monoclinic space groups $P2_1/n$ and $P2_1/c$, respectively, while the $Cs_2Hf_3Mn_3F_{20}$ phase crystallizes in the orthorhombic space group *Pmmn*. $Cs_2[M(H_2O)_6][Hf_2F_{12}]$ (M = Ni, Co, and Zn) exhibits a complex three dimensional (3D) crystal structure consisting of edge-sharing dimers of HfF_7 polyhedra, which are linked to the divalent metal octahedra via hydrogen bonding. $Cs_2Hf_3Mn_3F_{20}$ features corner-sharing HfF_7 and MnF_7 dimers as well as isolated MnF_6 octahedra, while the $CuHfF_6(H_2O)_4$ phase exhibits a 3D structure that consists of HfF_6 octahedra linked with neighboring copper octahedral units by hydrogen bonding interactions. UV-vis spectra of the titled compounds were collected and exhibit absorption bands due to electronic transitions in the divalent metal cations (Ni^{2+}, Co^{2+}, Cu^{2+}, and Mn^{2+}). Magnetic susceptibility measurements revealed paramagnetic behavior in the compounds containing the magnetic cations Ni, Co, Cu and Mn.

Introduction

The chemistry of the group 4 elements, specifically that of hafnium, has been of particular interest as it is relevant to electronic equipment, ceramics, control rods in nuclear reactors, light bulbs and in the making of superalloys.[1] Hafnium was identified in 1923[2] and, due to its late discovery, the interesting chemistry of hafnium containing materials has not been investigated as extensively as that of the other group 4 elements. Unlike titanium and zirconium, the hafnium atom contains a shell of 4f electrons that affects its chemical bonding with other atoms, slightly altering its behavior in certain types of chemical reactions. The perpetual importance of the nuclear reactor safety and the fundamental chemistry of inorganic hafnium fluorides motivated us to perform exploratory crystal growth in hafnium containing fluoride systems.

To date a small number of ternary hafnium containing fluorides, primarily alkali hafnium fluorides and some transition metal hafnium fluorides (e.g. $Ti_{0.5}Hf_{0.5}F_6$, $Ag_3Hf_2F_{14}$, $VHfF_6$), have been synthesized and their crystal structures reported in the literature.[3–10] Surprisingly, only a small number of quaternary hafnium containing fluorides have been deposited in the ICSD database.[11–21] Furthermore, no penternary and other extended series of hafnium containing fluorides have been reported in the literature so far. Considering the importance of hafnium as an element, the total number of alkali hafnium fluorides containing transition metals is remarkably low.

The interest in hafnium(IV) halides arises from their potential to create novel structural motifs and to observe specific physical properties. For example, the luminescent properties of the hafnium based alkali fluorides, Li_2HfF_6, $Na_5Hf_2F_{13}$, K_3HfOF_5 and $K_2Hf_3OF_{12}$, depend on a variety of factors including the alkali cation size, the presence or absence of oxygen in the compound, and the coordination environment of the hafnium atoms.[15] Similar effects have been observed in inorganic hybrid materials containing transition metal complex cations that exhibit efficient photocatalytic activity.[22–25] Hafnium halides, such as Cs_2HfCl_6 and Rb_2HfCl_6, exhibit a remarkable structural versatility, are promising materials for a number of optical applications, and have been shown to exhibit intrinsic luminescence along with excellent scintillation properties.[27–29] Kang and Biswas have investigated hafnium chlorides and employed quantum chemistry calculations to demonstrate

that the absorption and luminescence processes are highly dependent on the $[HfCl_6]^{2-}$ charge-transfer transition.[25] It is possible that similar processes could exist in $[HfF_6]^{2-}$ units.

In previous studies, the Hf(IV) containing fluorides were synthesized mostly via solid state routes, from saturated aqueous solutions, and under hydrothermal conditions. For example, the ternary and quaternary hafnium containing fluorides, such as $ScHf_3F_{15}$, $PdHfF_6$, $Ag_7Hf_6F_{31}$, $Cs_2Cu_3HfF_{12}$ and Li_2CaHfF_8, were obtained via solid state reactions involving heating the respective binary fluorides in either sealed Pt or Au tubes under dry Ar gas in a temperature range of 450–800 °C. [13,30–32] The anhydrous K_2HfF_6 and hydrated $KHfF_5{\cdot}H_2O$ were grown from saturated aqueous solutions containing HfF_4 and KF at room temperature (294 K) when present in the approximate molar ratios of 1:2 and 1:1, respectively.[33] The ternary alkali hafnium fluorides A_2HfF_6 (A = Rb, Cs), $Na_5Hf_2F_{13}$ and K_3HfF_7 were synthesized as high quality single crystals under supercritical hydrothermal conditions at 400–600°C.[34]

We recently determined that a large family of thorium containing fluorides can be grown under hydrothermal conditions as high-quality single crystals.[35–37] Although ThO_2 is usually thought of as a very inert and unreactive oxide, the use of concentrated HF coupled with elevated temperatures of hydrothermal reaction conditions allows ThO_2 digestion and results in highly stable thorium fluorides.[38] The well-known ability of hydrofluoric acid to readily digest even the most inert oxides potentially offers a similar convenient route for studying hafnium fluoride chemistry and also avoids a number of disadvantages that typically accompany the use of high temperature solid state routes for fluoride synthesis, such as oxide contamination; this issue is one reason for the scarcity of hafnium fluorides. Similar to thorium(IV) fluorides, an extended series of hafnium containing fluorides can be grown via a mild hydrothermal synthetic route as high quality single crystals. In this paper, we report on our efforts in using the mild hydrothermal method to prepare a new series of transition metal hafnium fluorides, $Cs_2[M(H_2O)_6][Hf_2F_{12}]$ (M= Ni, Co, and Zn), $CuHfF_6(H_2O)_4$, and quaternary $Cs_2Hf_3Mn_3F_{20}$ representing a significant increase in the number of known hafnium fluorides. We describe the synthesis, crystal structures, optical and magnetic properties of this series of hafnium(IV) containing divalent metal fluorides.

Experimental section

Reagents

CsF (Alfa Aesar, 99.9%), $CsCH_3COO$ (Alfa Aesar, 99%), HfO_2 (Alfa Aesar, 99.9%), $Co(CH_3COO)_2 \cdot 4H_2O$ (Alfa Aesar, 98%), $Ni(CH_3COO)_2 \cdot 4H_2O$ (Aldrich, 98%), $Zn(CH_3COO)_2 \cdot 2H_2O$ (Strem, 98%), $Cu(CH_3COO)_2 \cdot H_2O$ (Alfa Aesar, 99.9%) $Mn(CH_3COO)_2 \cdot 4H_2O$ (Alfa Aesar, 99.9%), and HF (EMD, 49%) were used as received.

Warning! HF should only be handled in a well ventilated space and proper safety precautions must be used. If contact with the liquid or vapor occurs, proper treatment procedures should immediately be followed.

Synthesis

Single crystals of the title compounds were grown using a mild hydrothermal route. For the preparation of $Cs_2[M(H_2O)_6][Hf_2F_{12}]$ (M= Co and Zn), 2 mmol of HfO_2, 4 mmol of CsF, and 1 ml of 49% HF were combined with 1 mmol of $Co(CH_3COO)_2 \cdot 4H_2O$ and $Zn(CH_3COO)_2 \cdot 2H_2O$, respectively. For the preparation of $Cs_2[Ni(H_2O)_6][Hf_2F_{12}]$, 2 mmol of HfO_2, 6 mmol of $CsCH_3COO$, and 1.5 ml of HF were combined with 1 mmol of $Ni(CH_3COO)_2 \cdot 4H_2O$. Similarly, for the preparation of $CuHfF_6(H_2O)_4$ and $Cs_2Hf_3Mn_3F_{20,}$ 2 mmol of CsF, 2 mmol of HfO_2, and 1 ml of HF were combined with 1 mmol of $Mn(CH_3COO)_2 \cdot 4H_2O$ and 1 mmol of $Cu(CH_3COO)_2 \cdot H_2O$, respectively. The respective solutions were placed into 23 ml PTFE-lined autoclaves. The autoclaves were sealed, heated to 200°C at a rate of 5 °C min^{-1}, held at this temperature for 24 hours, and cooled to room temperature at a rate of 6 °C h^{-1}. The mother liquor was decanted from the single crystal products, which were isolated by filtration and washed with methanol and acetone. In all cases, the reaction yielded a single phase product consisting of pink block crystals for Co, colorless plate crystals for Zn, light-green block crystals for Ni, and light blue-green plate crystals for Cu containing materials in nearly quantitative yield based on HfO_2. For $Cs_2Hf_3Mn_3F_{20,}$ colorless block crystals in an approximately 60% yield were obtained based on HfO_2. Reactions with Mg and Cd were also attempted using a number of different reaction

conditions, however no single crystals were obtained from these reactions. PXRD patterns of the products indicated no impurities (Figure S1–S4).

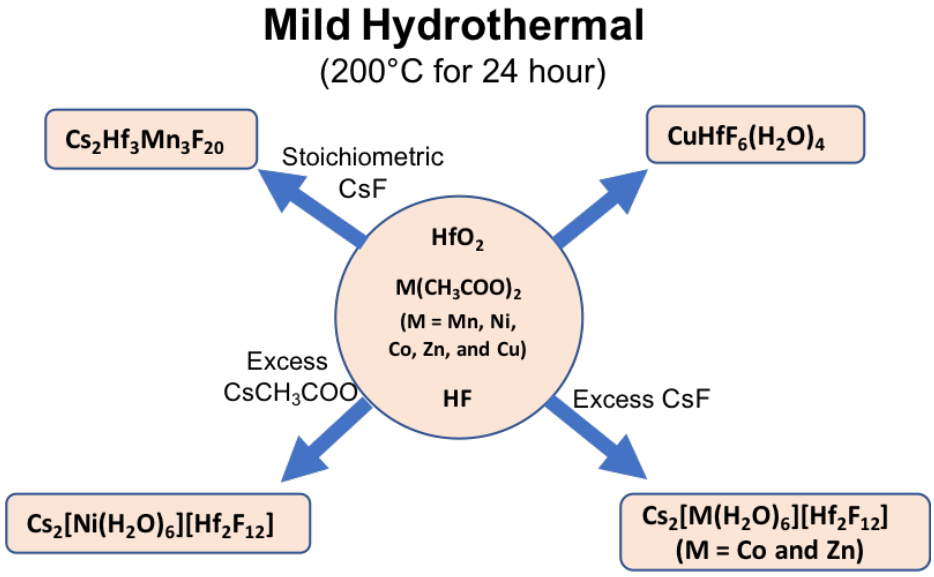

Figure 1. A schematic for the preparation of the hafnium containing fluorides with three different compositions, $Cs_2[M(H_2O)_6][Hf_2F_{12}]$ (M = Ni, Co, and Zn), $CuHfF_6(H_2O)_4$ and $Cs_2Hf_3Mn_3F_{20}$.

Single Crystal X-ray Diffraction

X-ray intensity data sets were collected at 300(2) K on a Bruker D8 QUEST diffractometer equipped with an Incoatec IμS 3.0 microfocus radiation source (Mo Kα, λ = 0.71073 Å) and a PHOTON II area detector. The crystals were mounted on a microloop with immersion oil. The raw area detector data frames were reduced and absorption corrections were performed using the SAINT and SADABS programs.[39,40] Initial structure solutions were obtained with SHELXS-2017 using direct methods. Full-matrix least-squares refinements against F^2 were performed with SHELXL software.[41] The hydrogen atoms of the water molecules in $Cs_2[M(H_2O)_6][Hf_2F_{12}]$ (M= Ni, Co, and Zn) were located from difference electron map and were refined with O-H distances restrained to 0.95 Å. All of the structures were checked for missing symmetry with the Addsym program implemented into PLATON software, and no higher symmetry was found.[42] $Cs_2[M(H_2O)_6][Hf_2F_{12}]$ (M= Ni, Co, and Zn) were found to be twins; the TwinRotMat algorithm

from PLATON software was employed to find a twin law (-1 0 0 0 -1 0 0.2 0 1), which was used along with MERG 0 and BASF instructions. All atoms were refined with anisotropic displacement parameters. The four unique hydrogen atoms in the structure of $CuHfF_6(H2O)_4$ were located in difference Fourier maps and refined freely. The crystallographic data and results of the diffraction experiments are summarized in Table 1.

Table 1. Crystallographic data for $Cs_2[M(H_2O)_6][Hf_2F_{12}]$ (M = Co, Ni, and Zn), $CuHfF_6(H_2O)_4$ and $Cs_2Hf_3Mn_3F_{20}$.

	$Cs_2[Co(H_2O)_6][Hf_2F_{12}]$	**$Cs_2[Ni(H_2O)_6][Hf_2F_{12}]$**	**$Cs_2[Zn(H_2O)_6][Hf_2F_{12}]$**	**$CuHfF_6(H_2O)_4$**	**$Cs_2Hf_3Mn_3F_{20}$**
Formula weight	1017.83	1017.61	1024.27	428.09	1346.11
Crystal system	monoclinic	monoclinic	monoclinic	monoclinic	orthorhombic
Space group, Z	$P2_1/n$, 2	$P2_1/n$, 2	$P2_1/n$, 2	$P2_1/c$, 2	$Pmmn$, 2
a, Å	6.9622 (2)	6.9515 (2)	6.9534 (2)	5.6519(3)	8.2393(4)
b, Å	10.4791 (2)	10.4517 (3)	10.4837 (3)	10.0291(6)	15.5640(6)
c, Å	11.7439 (3)	11.6772 (3)	11.7386 (3)	7.5345(4)	6.6443(3)
β, deg	94.0760 (10)	93.4362 (10)	93.6701 (10)	103.824(2)	90
V, $Å^3$	854.64 (4)	846.88 (4)	853.96 (4)	414.71(4)	852.04(7)
ρ_{calcd}, g/cm^3	3.955	3.991	3.983		5.247
Radiation (λ, Å)	MoK_α (0.71073)				
μ, mm^{-1}	17.409	17.700	17.856	15.155	24.752
T, K	300 (2)				
Crystal dim.,mm^3	0.14×0.04×0.03	0.14×0.04x0.03	0.20×0.04×0.03	0.080×0.080×0.05	0.08×0.06×0.04
2θ range, deg.	3.30 – 36.39	2.62 – 35.50	3.32 – 36.28	3.447 – 35.060	2.80 – 29.75
Reflections collected	86563	28685	62956	20024	5709
Data/restraints/ parameters	86563/6/133	28685/6/132	62956 /6/131	1827/0/75	1173/0/86
R_{int}	0.0414	0.0445	0.0343	0.0291	0.0281
Goodness of fit	1.044	1.030	1.027	1.064	1.031
$R_1(I > 2\sigma(I))$	0.0348	0.0309	0.0259	0.0136	0.0194
wR_2 (all data)	0.0842	0.0826	0.0654	0.0290	0.0488

Powder X-ray Diffraction

Powder X-ray diffraction (PXRD) data for phase purity confirmation were collected on polycrystalline samples obtained by grinding single crystals. Data were collected on a Bruker D2

PHASER diffractometer utilizing Cu Kα radiation. The data were collected from 10 to 65° 2θ with a step size of 0.04°.

Energy-Dispersive Spectroscopy (EDS)

EDS was performed on product single crystals using a Tescan Vega-3 SEM equipped with a Thermo EDS attachment. The SEM was operated in low-vacuum mode. Crystals were mounted on an SEM stud with carbon tape and analyzed using a 20 KV accelerating voltage and a 30 s accumulating time.

Optical Properties

UV−vis spectra were recorded in the diffuse reflectance mode using a PerkinElmer Lambda 35 UV/visible scanning spectrophotometer equipped with an integrating sphere. Diffuse reflectance spectra were recorded in the 200−900 nm range. Reflectance data were converted to absorbance by the instrument via the Kubelka−Munk function.[43] All optical measurements were performed on polycrystalline powders obtained by grinding the product single crystals.

Magnetism

Magnetic susceptibility measurements were performed on a Quantum Design MPMS 3 SQUID magnetometer. Field-cooled (FC) and zero-field-cooled (ZFC) magnetic susceptibility measurements were performed from 2 to 375 K in an applied field of 0.1 T. The raw data were corrected for radial offset and sample shape effects according to the method described in the literature.[44] All magnetic data were collected on polycrystalline powders obtained by grinding the product single crystals.

Results and Discussion

Crystal Growth

A mild hydrothermal technique offered a convenient route to synthesize a series of novel hafnium(IV) containing fluorides, $Cs_2[M(H_2O)_6][Hf_2F_{12}]$ (M = Ni, Co, and Zn), $CuHfF_6(H_2O)_4$ and $Cs_2Hf_3Mn_3F_{20}$, at the relatively low temperature of 200 °C. The conditions were optimized with respect to the molar ratios of the reactants, especially for the Cs precursor, to obtain phase

pure samples. Despite the similar sizes of the divalent cations in the studied series, Ni, Co, Zn and Cu containing compounds crystallize as hydrates, while the Mn-containing compound forms as an anhydrous fluoride. All attempts to obtain a hydrated Mn analog were unsuccessful, and simply resulted in the formation of $Cs_2Hf_3Mn_3F_{20}$ crystals.

HfO_2 is known to be inert and unreactive toward many acids and bases. The use of hydrofluoric acid achieves digestion of HfO_2 and thus enables its participation in the formation of fluoride compounds. In these reactions hydrofluoric acid plays the role of both a mineralizer and a fluorine source[45] that dissolve the starting materials and stabilize both the tetravalent hafnium and divalent transition metal ions in a fluoride matrix. During the preparation of $Cs_2[Ni(H_2O)_6][Hf_2F_{12}]$, we found that the use of $CsCH_3COO$ as a starting material at a low molar concentration results in the previously reported $HfNiF_6(H_2O)_6$ phase as the major product.[46] The reaction outcome can be shifted toward the target phase by using a three-fold molar excess of $CsCH_3COO$, which results in a phase pure sample of $Cs_2[Ni(H_2O)_6][Hf_2F_{12}]$. Interestingly, using copper acetate as a starting material and different molar ratios of cesium under similar reaction conditions yielded a different compound with the composition $CuHfF_6(H_2O)_4$. Although the compound has been reported in the literature[47] its crystal structure has not been deposited to ICSD. All of the products were obtained as high-quality single crystals in practically quantitative yield. The crystals of the hydrated phases are water-soluble, but can be stored in air for at least one month.

Structure Description

$Cs_2[M(H_2O)_6][Hf_2F_{12}]$ (M= Ni, Co and Zn)

All three $Cs_2[M(H_2O)_6][Hf_2F_{12}]$ (M= Ni, Co, and Zn) compounds are isostructural and exhibit only minor differences in their unit cell parameters, bond lengths, and bond angles. These compounds crystallize in the monoclinic space group $P2_1/n$ and the asymmetric unit contains one crystallographically unique hafnium, one cesium, one divalent metal, six fluorine, three oxygen, and six hydrogen atoms. The crystal structure is constructed of edge-sharing hafnium dimers (Figure 2a) linked to the metal octahedra (Figure 2b) through hydrogen-bonding. Large pores in the structure contain the cesium cations, which connect the metal building units into a three

dimensional structure (Figure 2c, d). The unit cell volumes in this isostructural series changes accordingly to the size of the divalent cation, i.e. the unit cell volume increases from 846.88(4) $Å^3$ for the Ni analog ($r(Ni^{2+})$ = 0.69 Å) to 854.64(4) and 853.96(4) $Å^3$ for Zn (0.74 Å) and Co (0.745 Å), respectively.[48]

The single unique hafnium site in the structure forms a HfF_7 coordination polyhedron in the shape of a pentagonal bipyramid. The two axial bonds of the bipyramid are slightly shorter, 1.956(4)–1.978(4) Å, than the five equatorial bonds, 2.027(4)–2.157(3) Å. Two HfF_7 polyhedra share an edge to form the hafnium dimer shown in Figure 1a. The metal cations M^{2+} = Co^{2+}, Ni^{2+}, and Zn^{2+} form almost regular octahedra with M–O bond lengths of 2.067(5)–2.125(4), 2.052(5)–2.062(4), and 2.093(4)–2.099(4) Å, respectively, and the O–M–O angles are within a narrow range of 88.29(19)–91.71(19)°. The $[Hf_2F_{12}]^{4-}$ dimers and $[M(H_2O)_6]^{2+}$ octahedra are held together by moderate hydrogen bonds between the water molecules of the octahedral complexes and the fluorine atoms of the dimers. Each dimer links to six different octahedra and vice versa, resulting in a hydrogen-bonded framework with a primitive cubic (**pcu**) topology.

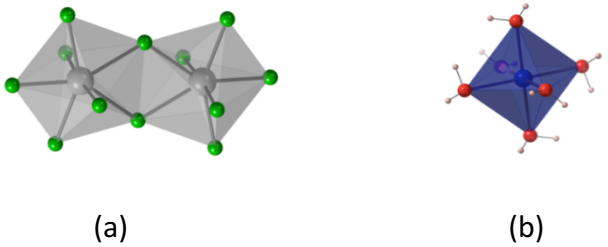

(a) (b)

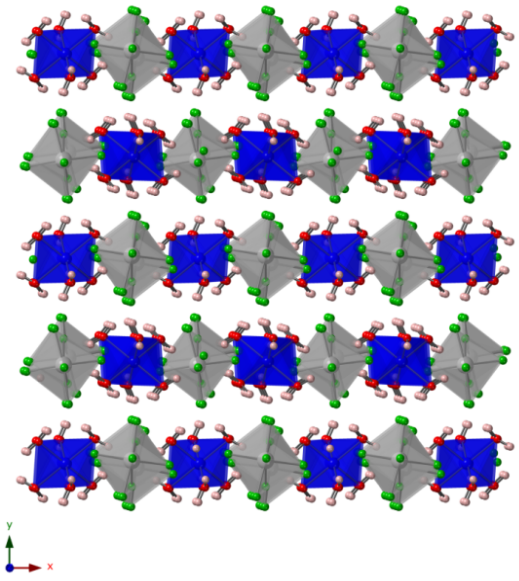

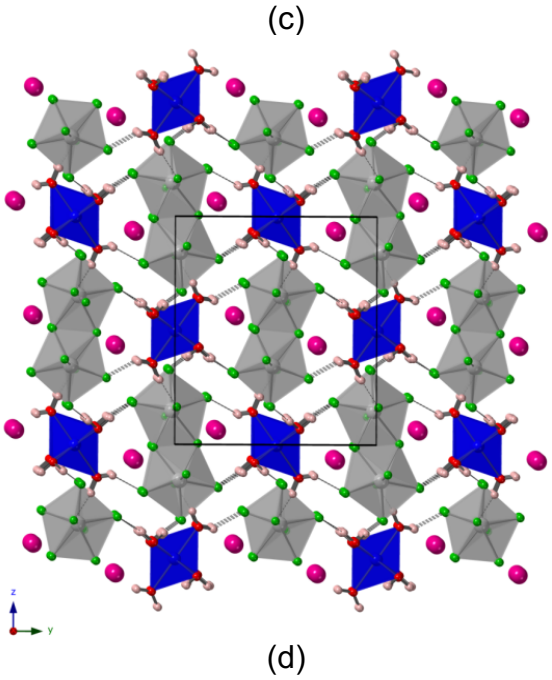

Figure 2. (a) Illustration of edge-sharing dimer of HfF_7 polyhedra, (b) metal ion (M = Ni, Co, and Zn) octahedron, and (c, d) a view of $Cs_2[M(H_2O)_6][Hf_2F_{12}]$ (M = Ni, Co, and Zn) structure along the *c* and *a* axes, respectively. The hafnium, cesium, M (M = Ni, Co, and Zn), oxygen, and fluorine atoms are shown in light grey, pink, deep blue, red, and green, respectively.

$CuHfF_6(H_2O)_4$

The compound crystallizes in the monoclinic $P2_1/c$ space group, which was uniquely determined by the pattern of systematic absences in the intensity data and confirmed by structure solution. The compound is isostructural with the zirconium analog, $CuZrF_6(H_2O)_4$.[49] The asymmetric unit consists of one Cu atom, one Hf atom, three fluorine atoms, two oxygen atoms of water molecules, and four hydrogen atoms. The structure is a framework consisting of 1D chains of $Cu(H_2O)_4$ units alternating with HfF_6 octahedra, which are further connected by hydrogen bonding interactions between the hydrogen atoms of the metal complex $[M(H_2O)_4]^{2+}$ and the fluoride ions of the hafnium site $[HfF_6]^{2-}$, resulting in the three dimensional structure shown in Figure 3.

The hafnium site forms a HfF_6 coordination polyhedron in the shape of an octahedron with Hf–F bonds ranging from 1.9772(11) to 2.0090(11) Å. The HfF_6 octahedra are linked to neighboring copper units through a Cu–F bond in an alternating fashion to form a 1D chain along the *c* axis. The Cu^{2+} cations are located in nearly regular octahedra with Cu–O bond lengths ranging from 1.9665(14) to 1.9724(13) Å and a Cu–F bond length of 2.2429(11) Å. The 1D chains are further linked to each other by O–H···F hydrogen bonds to form a three dimensional structure.

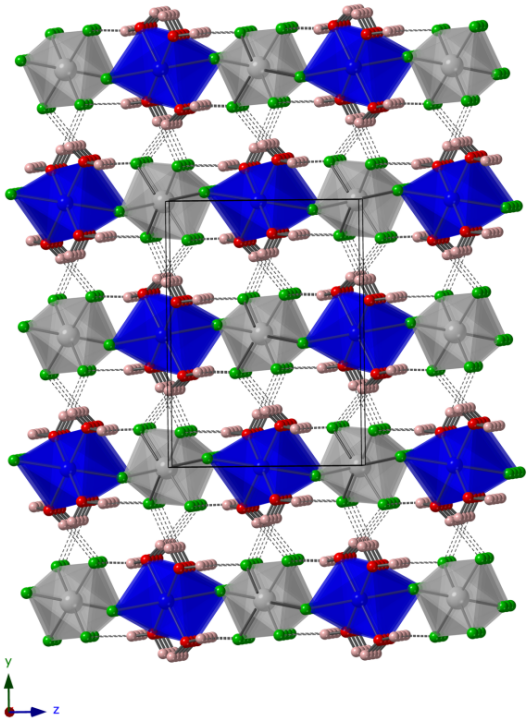

Figure 3. Illustration of the three dimensional crystal structure of $CuHfF_6(H_2O)_4$ along the *a* axis. The hafnium, copper, oxygen, and fluorine atoms are shown in light grey, deep blue, red, and green respectively.

$Cs_2Hf_3Mn_3F_{20}$

$Cs_2Hf_3Mn_3F_{20}$ crystallizes in the orthorhombic space group *Pmmn* and its asymmetric unit contains one Cs, two Hf, two Mn and ten F sites. The structure is a framework that consists of corner- and edge-sharing hafnium and manganese polyhedra that create channels in which the cesium cations are located. Both unique hafnium sites form HfF_7 coordination polyhedra, (Figure 4a), in the shape of an almost regular pentagonal bipyramid with Hf–F bonds ranging from 1.988(4) to 2.241(4) Å.

In both $Hf(1)F_7$ and $Hf(2)F_7$ bipyramids, the axial bonds are slightly shorter than the equatorial ones. The Hf(1) site has C_{2V} site symmetry, while the Hf(2) sites are located at a mirror plane. Unlike the Hf1 site, which shares corners and edges exclusively with the manganese polyhedra, Hf(2) polyhedra share one corner with each other to form a dimer, (Figure 4b), with a parallel alignment of the equatorial planes. There are two crystallographically unique manganese atoms present in the structure. Mn(1) atoms form an uncommon $Mn(1)F_7$ pentagonal bipyramid, which previously were observed in only five inorganic manganese fluorides, $CrMnF_5$, $NaBa(Mn_3F_{11})$, $Mn(BF_4)_2$, $RbMnZrF_7$, and $TlMnZrF_7$,[50–53] whereas Mn(2) exhibits a more typical distorted octahedral environment (Figure 3c, d). As expected, the Mn–F bond lengths in the pentagonal bipyramids are slightly elongated as compared to the octahedral sites, 2.120(3)–2.260(3) vs. 2.066(3)–2.139(4) Å, respectively. Despite this difference, the volumes of the manganese atoms' Voronoi polyhedra are almost the same, 9.53 and 9.27 $Å^3$ for Mn1 and Mn2, respectively.[54] $Mn(1)F_7$ polyhedra share three corners and two edges with five hafnium atoms, whereas $Mn(2)F_6$ octahedra corner share all six fluorine atoms. The equatorial planes of all four unique metal atom sites are arranged in parallel, resulting in pseudo-layers in the *bc* plane, shown in Figure 5a. The layers are linked to each other through the axial F atoms, which consecutively connect alternating Mn and Hf atoms from different layers into the 3D framework shown in Figure 4e. The cesium cations reside in the framework channels, which run along the *a* axis, and form multiple interactions with the F atoms. Attempts to replace the Cs with Na cations via ion exchange using an aqueous NaCl solution resulted in the decomposition of $Cs_2Hf_3Mn_3F_{20}$. The underlying net of the framework has a **btu** topology according to the classification performed with TOPOS software, as shown in figure S6.[55]

The flat pseudolayers in the structure of $Cs_2Hf_3Mn_3F_{20}$ closely resemble the structure of $NaHf_2VF_{11}$,[4] which consists of one Hf and one V site. In both structures, the layers are composed of $MnHfF_8$ or Hf_2F_8 edge-sharing dimers, which are connected into chains by corner sharing (Figure 5). In both cases, the chains are linked together by either HfF_7 and MnF_6 or VF_6 polyhedra for $Cs_2Hf_3Mn_3F_{20}$ and $NaHf_2VF_{11}$, respectively. It is interesting that the interchain V and Mn atoms adopt an octahedral environment, unlike the interchain Hf atoms that manifest their larger size in a tendency to take on a higher coordination number. The resultant HfF_7 pentagonal bipyramids that draw an additional fluorine atom to their equatorial plane from the pentagonal bipyramidal

manganese atoms, causing a slight distortion of otherwise linear M-F-M fragment. Unlike Hf, the V atoms form a preferable octahedral environment by corner sharing with the polyhedra from the chains. In $Cs_2Hf_3Mn_3F_{20}$, the pseudolayers stack one on another by corner sharing the axial fluorine atoms, whereas in $NaHf_2VF_{11}$ the layers are shifted one along another in the direction perpendicular to the dimer chains. Close resemblance of the layers coupled with the structural diversity stemming from the size of the cations suggests additional synthetic directions using the concept of compositional design of new magnetic materials.

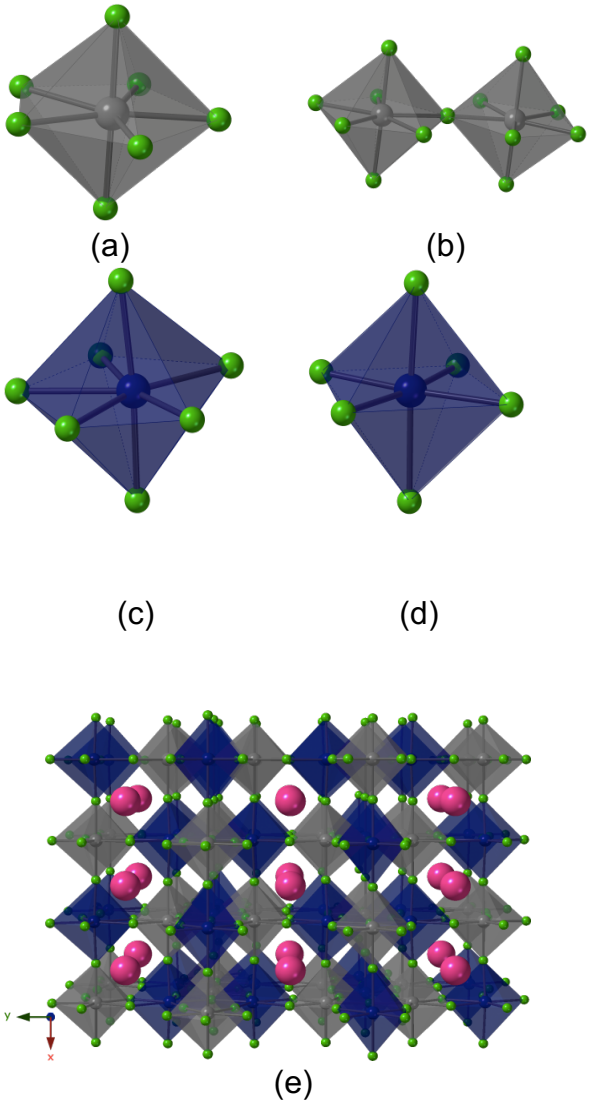

Figure 4. (a) Illustration of a $Hf(1)F_7$ coordination polyhedron, (b) a $Hf(2)F_7$ corner-sharing dimer of, (c) $Mn(1)F_7$ trigonal bipyramid, (d) $Mn(2)F_6$ octahedron, and (e) a view of the 3D structure of $Cs_2Hf_3Mn_3F_{20}$ along the *c* axis. The hafnium, cesium, manganese, and fluorine atoms are shown in light grey, pink, deep blue, and green, respectively.

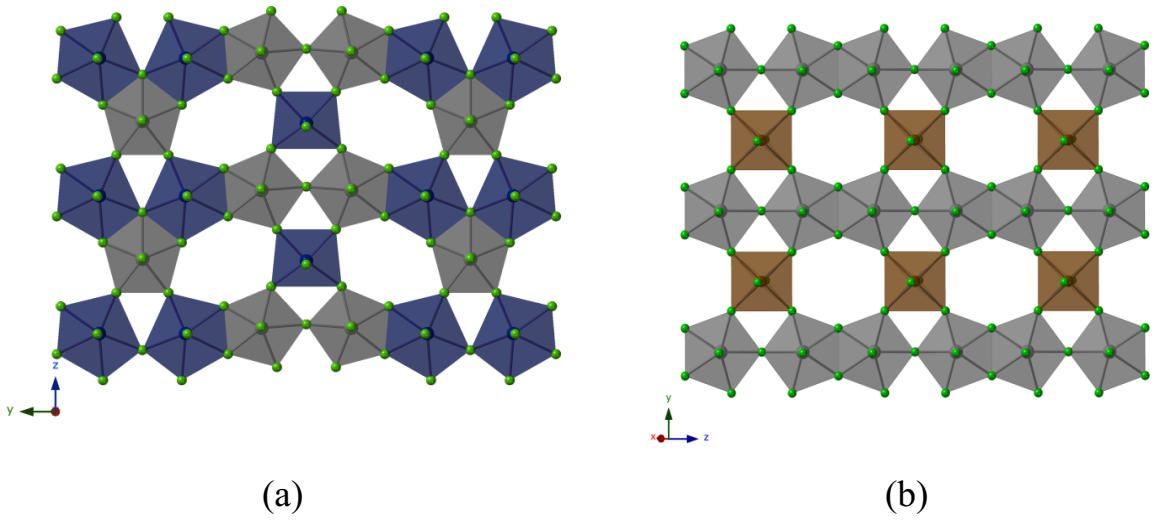

Figure 5. A view of flat pseudolayers in the structures of (a) $Cs_2Hf_3Mn_3F_{20}$ and (b) $NaHf_2VF_{11}$. The hafnium, manganese, and vanadium atoms are shown in light grey, blue, and brown respectively.

UV-Vis Diffuse Reflectance Spectroscopy

UV-Vis diffuse reflectance data were collected on ground crystals of the reported materials, $Cs_2[M(H_2O)_6][Hf_2F_{12}]$ (M = Ni and Co), $CuHfF_6(H_2O)_4$ and $Cs_2Hf_3Mn_3F_{20}$. The normalized UV-vis spectra for these compounds (Figure S7) exhibit absorption bands due to the d-d electronic transitions in the divalent metal ions interpreted by the Tanabe-Sugano diagram.[56] The cobalt analog shows weak absorption peaks at 258 and 296 nm, along with a broad intense absorption band at 511 nm, which were attributed to $^3T_{2g}$ (F), $^3A_{2g}$ (F) and $^3T_{1g}$ (P) transitions from the $^3T_{1g}$ ground state. Similarly, the nickel analog displays three broad absorption bands at 398, 653, and 721 nm, which are due to transitions from the $^3A_{2g}$ ground state to $^3T_{1g}$ (F), $^3T_{2g}$ (F) and $^3T_{1g}$ (P) excited states. In the case of $Cs_2Hf_3Mn_3F_{20}$, the optical absorption spectra of Mn^{2+} ions have spin forbidden transitions, and only one weak absorption band is observed around 390 nm. The copper-

containing sample displays an intense broad absorbance with a maximum at 621 nm due to ^2E_g to $^2T_{2g}$ transition in the Cu^{2+} cation.

Magnetic Properties

The magnetic susceptibility data for the hafnium fluorides with magnetic ions, $Cs_2[M(H_2O)_6][Hf_2F_{12}]$ (M = Ni and Co), $Cs_2Hf_3Mn_3F_{20}$, and $CuHfF_6(H_2O)_4$, were collected over the temperature range of 2–375 K, as shown in Figure 6. All four compounds exhibit Curie-Weiss behavior between 100 and 375 K. The inverse susceptibility data range were fitted to determine the effective magnetic moments and the Weiss constants; the data are summarized in Table 2 along with the expected values that were calculated for the free ions.

The effective magnetic moments for Mn, Ni, and Cu containing compounds are 6.21, 3.28, and 1.98 μ_B, respectively, all slightly higher than the calculated values for free ions, 5.92, 2.83, and 1.73 μ_B. Both overlapping zero-field and field cooled magnetic susceptibility curves (Figure S8) for $Cs_2[Ni(H_2O)_6][Hf_2F_{12}]$ exhibit a small kink at 68-71 K, which might be indicative of a magnetic or structural transition in the target phase or the presence of a magnetic impurity. One possible source of a magnetic impurity is nickel fluoride, which undergoes an antiferromagnetic transition at ~69 K and which falls precisely into the range of the observed transition. The Curie-Weiss law fit for $Cs_2[Co(H_2O)_6][Hf_2F_{12}]$ yields a moment of 4.78 μ_B that is significantly higher than the calculated value for a free ion, 3.87 μ_B. It nonetheless falls into the known range of experimentally observed moments, suggesting the presence of spin-orbit coupling to result in the higher moment.

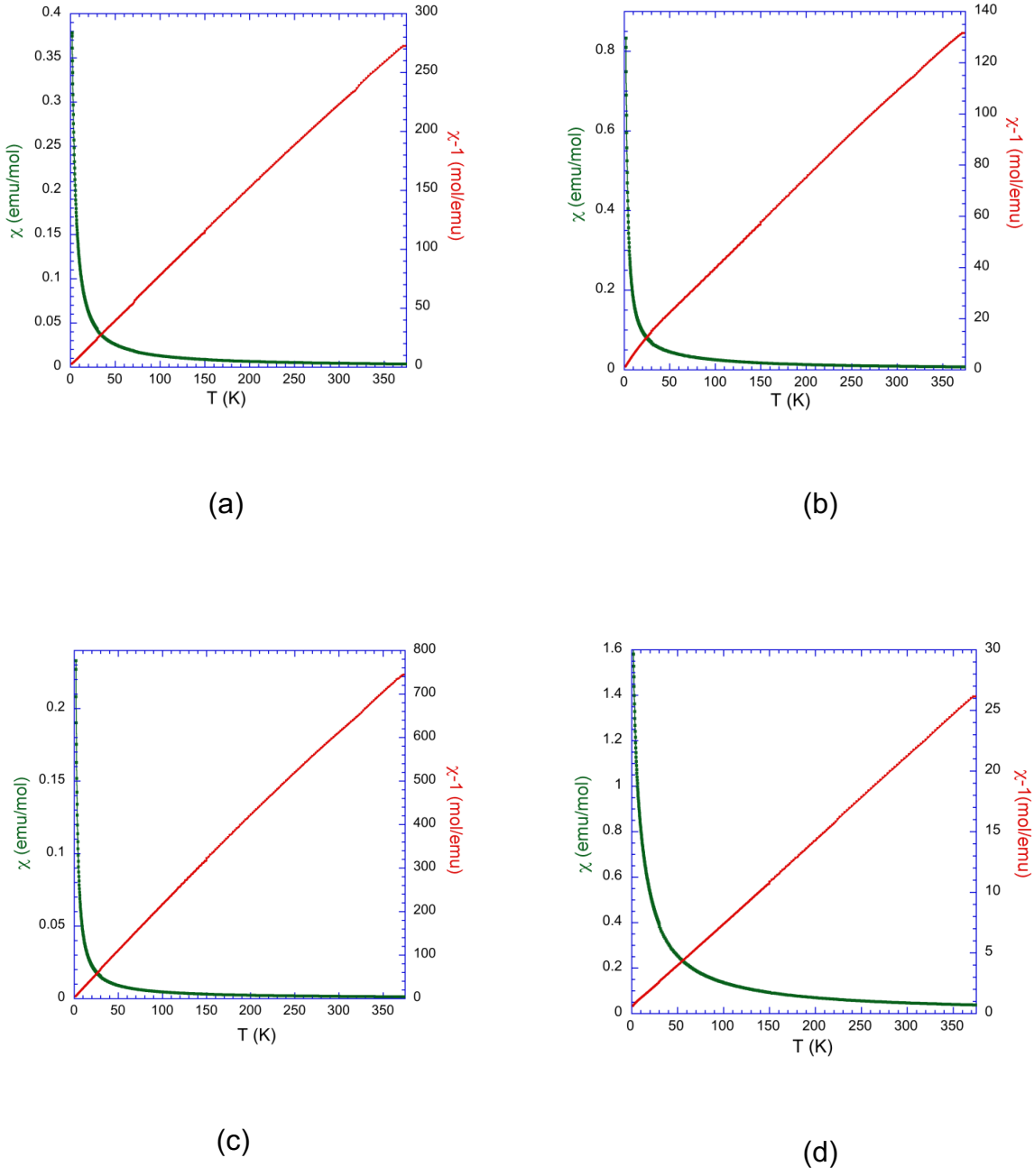

Figure 6. Magnetic susceptibility and inverse susceptibility plot of (a) $Cs_2[Ni(H_2O)_6][Hf_2F_{12}]$ (b) $Cs_2[Co(H_2O)_6][Hf_2F_{12}]$ (c) $CuHfF_6(H_2O)_4$ and (d) $Cs_2Hf_3Mn_3F_{20}$. Data were collected in a ZFC measurement with a 0.1 T applied magnetic field and are shown in the range from 2 to 375 K.

Table 2. Curie – Weiss Constants and Effective magnetic moments for the hafnium fluorides

Compound	θ (K)	μ_{eff}/μ_B	μ_{calc}/μ_B
$Cs_2[Ni(H_2O)_6][Hf_2F_{12}]$	-2.6	3.28	2.83
$Cs_2[Co(H_2O)_6][Hf_2F_{12}]$	-9.4	4.78	3.87
$Cs_2Hf_3Mn_3F_{20}$	-4.9	6.21	5.92
$CuHfF_6(H_2O)_4$	-3.4	1.98	1.73

Conclusion

In this paper we described the synthesis and characterization of a new series of hafnium(IV) containing fluorides $Cs_2[M(H_2O)_6][Hf_2F_{12}]$ (M= Ni, Co, and Zn), $CuHfF_6(H_2O)_4$, and $Cs_2Hf_3Mn_3F_{20}$. A mild hydrothermal synthetic route was employed for the synthesis and resulted in three different compositions. The compounds $Cs_2[M(H_2O)_6][Hf_2F_{12}]$ (M= Ni, Co, and Zn) and $Cs_2Hf_3Mn_3F_{20}$ exhibit a complex three-dimensional crystal structure, in which the Hf^{4+} cation is found in a seven-fold coordination environment, forming a hafnium dimer. UV-vis data are consistent with the +2 oxidation state for the divalent metal ions in $Cs_2[M(H_2O)_6][Hf_2F_{12}]$ (M= Ni and Co), $CuHfF_6(H_2O)_4$, and $Cs_2Hf_3Mn_3F_{20}$. The compounds containing Ni^{2+}, Co^{2+}, Cu^{2+}, and Mn^{2+} ions exhibit paramagnetic behavior down to 2 K. All phases show an effective magnetic moment that is slightly higher than the calculated ones, although they fall into a range of experimentally observed magnetic moments. A possible explanation for the magnetic moment in $Cs_2Hf_3Mn_3F_{20}$ phase is the potential presence of a two different coordination environment of magnetic manganese atoms and its substantial number per formula unit.

Acknowledgements

Financial support for this work was provided by the National Science Foundation under DMR-1806279 and is gratefully acknowledged.

Supporting Information

PXRD patterns, UV-Vis Spectra, EDS results and magnetic susceptibility versus temperature plots. CSD 1917603-1917607 contain the supplementary crystallographic data for this paper. The data can be obtained free of charge from The Cambridge Crystallographic Data Centre via www.ccdc.cam.ac.uk/structures.

References

(1) Larsen, E. M. Zirconium and hafnium chemistry. Adv. *Inorg. Chem. Radiochem.* **1970**, 1-133.

(2) Coster, D.; v. Hevesy, G. The element of atomic number 72. *Naturwissenschaften* **1923**, *11*, 133-133.

(3) Mueller, B. G. New ternary silver(II) fluorides: $Ag_3MIV_2F_{14}$ (MIV = zirconium, hafnium). *Z. Anorg. Allg. Chem.* **1987**, *553*, 196-204.

(4) Schmidt, R.; Kraus, M.; Mueller, B. G. New fluorozirconates and -hafnates with V^{2+} and Ti^{2+}. *Z. Anorg. Allg. Chem.* **2001**, *627*, 2344-2350.

(5) Bode, H.; Teufer, G. Structures of hexafluozirconates and hexafluohafnates. *Z. Anorg. Allg. Chem.* **1956**, *283*, 18-25.

(6) Koller, D.; Mueller, B. G. Synthesis and structure of $RbHfF_5$, $Rb_2Zr_3F_{12}O$, and $Rb_2Hf_3F_{12}O$. Two oxyfluorides with central trigonal-plane [M_3O] group. *Z. Anorg. Allg. Chem.* **2002**, *628*, 575-579.

(7) Harris, L. A. The crystal structures of Na_3ZrF_7 and Na_3HfF_7. *Acta Crystallogr.* **1959**, *12*, 172.

(8) Granzin, J.; Saalfeld, H. Crystal structure refinement of tripotassium heptafluorohafnate(IV) and the disorder of the heptafluorohafnate complex. *Z. Kristallogr.* **1988**, *183*, 71−76.

(9) Saalfeld, H.; Guse, W. The polymorphism of K_2HfF_6. *Neu Jb. Mineral, Abh.* **1983**, *146*, 29-40.

(10) Neumann, C.; Saalfeld, H.; Gerdau, E.; Guse, W. Crystal structure refinement of dipotassium hexafluorohafnate (K_2HfF_6). *Z. Kristallogr.* **1986**, *175*, 159-164.

(11) Mueller, M.; Mueller, B. G. The crystal structure of $KPdMIVF_7$ (MIV = Zr, Hf). *Z. Anorg. Allg. Chem.* **1995**, *621*, 1047-1052.

(12) Graudejus, O.; Mueller, B. G. Ag^{2+} in trigonal-bipyramidal surrounding new fluorides with divalent silver $AgMII_3MIV_3F_{20}$ (MII = Cd, Ca, Hg; MIV = Zr, Hf). *Z. Anorg. Allg. Chem.* **1996**, *1996*, 1549-1556.
(13) Ayala, A.; Paschoal, C. W. A.; Gesland, J. Y.; Ellena, J.; Castellano, E. E.; Moreira, R. L. Single-crystal structure determination and infrared reflectivity study of the Li_2CaHfF_8 scheelite. *J. Phys.: Condens. Matter* **2002**, *14*, 5485-5495.
(14) Davidovich, R. L.; Pushilin, M. A.; Logvinova, V. B.; Gerasimenko, A. V. Crystal structure of monoclinic modifications of zirconium and hafnium tetrafluoride trihydrates. *J. Struct. Chem.* **2013**, *54*, 541-546.
(15) Underwood, C. C.; McMillen, C. D.; Chen, H.; Anker, J. N.; Kolis, J. W. Hydrothermal Chemistry, Structures, and Luminescence Studies of Alkali Hafnium Fluorides. *Inorg. Chem.* **2013**, *52*, 237-244.
(16) Hall, D.; Rickard, C. E. F.; Waters, T. N. The crystal structure of catena-di-μ-fluorodifluorodiaquohafnium(IV) monohydrate, $HfF_4.3H_2O$. *J. Inorg. Nucl. Chem.* **1971**, *33*, 2395-2401.
(17) Plitzko, C. Ph.D. Dissertation, Hannover University, Hannover, Germany, 1996.
(18) Plitzko, C.; Meyer, G. Single crystals of $(NH_4)ZrF_5$ and $(NH_4)HfF_5$ by oxidation of zirconium and hafnium with $(NH_4)HF_2$. *Z. Anorg. Allg. Chem.* **1998**, *624*, 169-170.
(19) Plitzko, C.; Strecker, M.; Meyer, G. Synthesis and crystal structure of the Fluoride ammoniacate $Zr(NH_3)F_4$ and $Hf(NH_3)F_4$. *Z. Anorg. Allg. Chem.* **1997**, *623*, 79-83.
(20) Kraus, F.; Baer, S. A.; Fichtl, M. B. The Reactions of Silver, Zirconium, and Hafnium Fluorides with Liquid Ammonia: Syntheses and Crystal Structures of $Ag(NH_3)2F{\cdot}2NH_3$, $[M(NH_3)4F_4]{\cdot}NH_3$(M = Zr, Hf), and $(N_2H_7)F$. *Eur. J. Inorg. Chem.* **2009**, *3*, 441-447.
(21) Kraus, M.; Muller, B. G. $KCuMIVF_7$ (MIV = Zr^{4+}, Hf^{4+}) a new type of structure. *Z. Anorg. Allg. Chem.* **2000**, *626*, 1929-1933.
(22) Yue, C.-Y.; Lei, X.-W.; Han, Y.-F.; Lu, X.-X.; Tian, Y.-W.; Xu, J.; Liu, X.-F.; Xu,-X. Transition-Metal-Complex Cationic Dyes Photosensitive to Two Types of 2D Layered Silver Bromides with Visible-Light-Driven Photocatalytic Properties. *Inorg. Chem.* **2016**, *55*, 12193-12203.
(23) Lei, X.-W.; Yue, C.-Y.; Zhao, J.-Q.; Han, Y.-F.; Yang, J.-T.; Meng, R.-R.; Gao, C.-S.; Ding, H.; Wang, C.-Y.; Chen, W.-D.; Hong, M.-C. Two Types of 2D Layered Iodoargentates Based on Trimeric $[Ag_3I_7]$ Secondary Building Units and Hexameric $[Ag_6I_{12}]$ Ternary Building Units: Syntheses, Crystal Structures, and Efficient Visible Light Responding Photocatalytic Properties. *Inorg. Chem.* **2015**, *54*, 10593-10603.
(24) Lei, X.-W.; Yue, C.-Y.; Wei, J.-C.; Li, R.-Q.; Mi,-F. Q.; Li, Y.; Gao, L.; Liu, Q.-X. Novel 3D Semiconducting Open-Frameworks based on Cuprous Bromides with Visible Light Driven Photocatalytic Properties. *Chem. Eur. J.* **2017**, *23*, 14547-14553.
(25) Yue, C.-Y.; Yue, Y.-D.; Sun, H.-X.; Li, D.-Y.; Lin, N.; Wang, X.-M.; Jin, Y.-X.; Dong, Y.-H.; Jing, Z.-H.; Lei, X.-W. Transition metal complex dye-sensitized 3D iodoplumbates: syntheses, structures and photoelectric properties. *Chem. Commun.* **2019**, *55*, 6874-6877.
(26) Saeki, K.; Fujimoto, Y.; Koshimizu, M.; Yanagida, T.; Asai, K. Comparative study of scintillation properties of $Cs_2HfCl_6$and Cs_2ZrCl_6. *Appl. Phys. Express* **2016**, *9*, 042602.
(27) Burger, A.; Rowe, E.; Groza, M.; Morales Figueroa, K.; Cherepy, N. J.; Beck, P. R.; Hunter, S.; Payne, S. A. Cesium hafnium chloride: A high light yield, non-hygroscopic cubic crystal scintillator for gamma spectroscopy. *Appl. Phys. Lett.* **2015**, *107*, 143505.

(28) Saeki, K.; Wakai, Y.; Fujimoto, Y.; Koshimizu, M.; Yanagida, T.; Nakauchi, D.; Asai, K. Luminescence and scintillation properties of Rb_2HfCl_6 crystals. *Jpn. J. Appl. Phys.* **2016**, *55*, 110311.
(29) Kang, B.; Biswas, K. Carrier Self-trapping and Luminescence in Intrinsically Activated Scintillator: Cesium Hafnium Chloride (Cs_2HfCl_6). *J. Phys. Chem. C* **2016**, *120*, 12187-12195.
(30) Fedorov, P. P.; Pil'gun, O. V.; Sobolev, B. P.; Fedorov, P. I. Preparation of scandium hafnium fluoride. *Zh. Neorg. Khim.* **1990**, *35*, 1068-1069.
(31) Ruchaud, N.; Grannec, J.; Tressaud, A. Polymorphic and magnetic study of ternary palladium (II) fluorides $PdMIVF_6$ (MIV = Zr, Sn, Hf). *J. Alloys Compd.* **1994**, *205*, 17-20.
(32) Koller, D.; Mueller, B. G. Synthesis and structure of $Ag_7M_6F_{31}$ (M = Zr, Hf, Ce). *Z. Anorg. Allg. Chem.* **2000**, *626*, 1426-1428.
(33) Mueller, M.; Mueller, B. G. The crystal structure of $KPdMIVF_7$ (MIV = Zr, Hf). *Z. Anorg. Allg. Chem.* **1995**, *621*, 993-1000.
(34) Neumann, C.; Granzin, J.; Saalfeld, H. Crystal structure and optical properties of potassium pentafluorohafnate monohydrate, $KHfF_5 \cdot H_2O$. *Z. Kristallogr.* **1988**, *184*, 221-227.
(35) Klepov, V. V.; Felder, J. B.; zur Loye, H.-C. Synthetic Strategies for the Synthesis of Ternary Uranium(IV) and Thorium(IV) Fluorides. *Inorg. Chem.* **2018**, *57*, 5597-5606.
(36) Klepov, V. V.; Morrison, G.; zur Loye, H.-C. $Na_nMTh_6F_{30}$: A Large Family of Quaternary Thorium Fluorides. *Cryst. Growth Des.* **2019**, *19*, 1347-1355.
(37) Klepov, V. V.; Pace, K. A.; Calder, S.; Felder, J. B.; zur Loye, H.-C. 3d-Metal Induced Magnetic Ordering on U(IV) Atoms as a Route toward U(IV) Magnetic Materials. *J. Am. Chem. Soc.* **2019**, *141*, 3838-3842.
(38) Mann, M.; Thompson, D.; Serivalsatit, K.; Tritt, T. M.; Ballato, J.; Kolis, J. W. Hydrothermal Growth and Thermal Property Characterization of ThO_2 Single Crystals. *Cryst. Growth Des.* **2010**, *10*, 2146-2151.
(39) *SAINT*; Bruker AXS Inc.: Madison, WI, USA, 2012.
(40) Krause, L.; Herbst-Irmer, R.; Sheldrick, G. M.; Stalke, D. Comparison of silver and molybdenum microfocus X-ray sources for single-crystal structure determination. *J. Appl. Crystallogr.* **2015**, *48*, 3-10.
(41) Sheldrick, G. M. Crystal structure refinement with SHELXL. *Acta Crystallogr., Sect. C: Struct. Chem.* **2015**, *71*, 3-8.
(42) Spek, A. L. Structure validation in chemical crystallography. *Acta Crystallogr., Sect. D: Biol. Crystallogr.* **2009**, *65*, 148-155.
(43) Kubelka, P.; Munk, F. A contribution to the look of the paints. *Z. Technol. Phys.* **1931**, *12*, 593.
(44) Morrison, G.; zur Loye, H.-C. Simple correction for the sample shape and radial offset effects on SQUID magnetometers: Magnetic measurements on Ln_2O_3 (Ln=Gd, Dy, Er) standards. *J. Solid State Chem.* **2015**, *221*, 334-337.
(45) Yeon, J.; Smith, M. D.; Morrison, G.; zur Loye, H.-C. Trivalent cation-controlled phase space of new U(IV) fluorides, $Na_3MU_6F_{30}$ ($M = Al^{3+}$, Ga^{3+}, Ti^{3+}, V^{3+}, Cr^{3+}, Fe^{3+}): mild hydrothermal synthesis including an in situ reduction step, structures, optical, and magnetic properties. *Inorg. Chem.* **2015**, *54*, 2058-2066.
(46) Halasyamani, P.; Willis, M. J.; Stern, C. L.; Poeppelmeier, K. R. Crystal growth in aqueous hydrofluoric acid and $(HF)_x \cdot$pyridine solutions: syntheses and crystal structures of

$[Ni(H_2O)_6]^{2+}[MF_6]^{2-}$ (M = Ti, Zr, Hf) and $Ni_3(py)_{12}F_6 \cdot 7H_2O$. *Inorg. Chim. Acta* **1995**, *240*, 109-115.

(47) Fischer, J.; De Cian, A.; Weiss, R. Stereochemistry of copper(II) in fluoride and oxofluoride complexes of copper(II). I. Structural study of compounds of the type: $CuMF_6.4H_2O$, $CuMOF_5.4H_2O$, and $CuMO_2F_4.4H_2O$. *Bull. Soc. Chim. Fr.* **1966**, *8*, 2646-2647.

(48) Shannon, R. D. Revised effective ionic radii and systematic studies of interatomic distances in halides and chalcogenides. *Acta Crystallogr., Sect. A: Cryst. Phys., Diffr., Theor. Gen. Crystallogr.* **1976**, *32*, 751-767.

(49) Fischer, J.; Weiss, R. Stereochemistry of zirconium and copper in the hydrated copper fluorozirconates. I. Crystal structure of copper hexafluorozirconate tetrahydrate. *Acta Crystallogr. B Struct. Cryst. Cryst. Chem.* **1973**, *29*, 1955-1957.

(50) Cockman, R. W.; Hoskins, B. F.; McCormick, M. J.; O'Donnell, T. A. Isolation and crystal structure of manganese(II) tetrafluoroborate: a unique example of manganese(II) with seven unidentate ligands. *Inorg. Chem.* **1988**, *27*, 2742-2745.

(51) El-Ghozzi, M.; Avignant, D.; Guillot, M. Synthesis, Structures, and Characterization of $MMnZrF_7$ (M = Tl, Rb, NH_4, K) Fluorides: An Example of 7-Coordination of Divalent Manganese. *J. Solid State Chem.* **1994**, *108*, 51-58.

(52) Férey, G.; de Pape, R.; Poulain, M.; Grandjean, D.; Hardy, A. The crystalline structure of $MnCrF_5$. *Acta Crystallogr., Sect. B: Struct. Crystallogr. Cryst. Chem.* **1977**, *33*, 1409-1413.

(53) Darriet, J.; Ducau, M.; Feist, M.; Tressaud, A.; Hagenmuller, P. Crystal structure and magnetic properties of $NaBa_2Mn_3F_{11}$: A new layer-type fluoride compound. *J. Solid State Chem.* **1992**, *98*, 379-385.

(54) Blatov, V. A.; Shevchenko, A. P.; Serezhkin, V. N. Crystal space analysis by means of Voronoi-Dirichlet polyhedra. *Acta Crystallogr., Sect. A: Found. Crystallogr.* **1995**, *51*, 909-916.

(55) O'Keeffe, M.; Peskov, M. A.; Ramsden, S. J.; Yaghi, O. M. The Reticular Chemistry Structure Resource (RCSR) database of, and symbols for, crystal nets. *Acc. Chem. Res.* **2008**, *41*, 1782-1789.

(56) Tanabe, Y.; Sugano, S. On the Absorption Spectra of Complex Ions, III The Calculation of the Crystalline Field Strength. *J. Phys. Soc. Jpn.* **1956**, *11*, 864-877.

For Table of Content use only

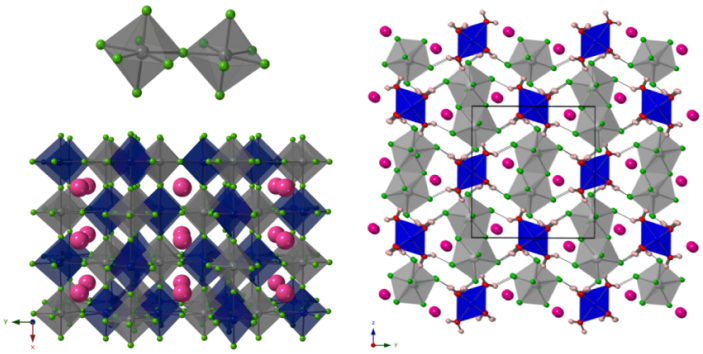

A view of the corner sharing hafnium dimer and the 3D crystal structure of $Cs_2Hf_3Mn_3F_{20}$ along the *c* axis and the figure on the right is the 3D structure of $Cs_2[M(H_2O)_6][Hf_2F_{12}]$ (M= Ni, Co, and Zn) along the *a* axis.